Available online at www.sciencedirect.com
ScienceDirect
Acta Materialia 56 (2008) 2718–2727
Acta MATERIALIA
www.elsevier.com/locate/actamat

Stress-driven migration of grain boundaries and fracture processes in nanocrystalline ceramics and metals

I.A. Ovid'ko [a,*], A.G. Sheinerman [a], E.C. Aifantis [b]

[a] *Institute for Problems of Mechanical Engineering, Russian Academy of Sciences, Bolshoj 61, Vas. Ostrov, St. Petersburg 199178, Russia*
[b] *Aristotle University of Thessaloniki, 54124 Thessaloniki, Greece*

Received 13 September 2007; received in revised form 19 January 2008; accepted 3 February 2008
Available online 14 March 2008

Abstract

Theoretical models are suggested that describe the effects of stress-driven migration of grain boundaries (GBs) on both the formation of nanoscale cracks (nanocracks) and the growth of comparatively large cracks in deformed nanocrystalline ceramics and metals. The GB migration under consideration is driven by the applied stress, carries plastic flow and produces quadrupoles of disclination defects in nanocrystalline materials. The disclinations create high local stresses capable of initiating the formation of nanocracks. In this paper, the conditions at which the formation of nanocracks is energetically favorable are theoretically described. The external stress values needed to initiate nanocrack formation near the disclinations in nanocrystalline metals (Al and Ni) with the finest grains and nanoceramics (Al_2O_3) are estimated. In addition, we estimated the effect of the stress-driven migration of GBs on the growth of pre-existing, comparatively large cracks in nanocrystalline Ni with the finest grains.

Keywords: Grain boundary migration; Disclinations; Fracture; Nanocrystalline microstructure; Modelling

1. Introduction

Nanocrystalline ceramic and metallic materials exhibit outstanding mechanical properties due to the nanoscale and interface effects [1–6]. In particular, interfaces – grain and interphase boundaries – crucially influence plastic flow and fracture processes in nanocrystalline materials (NCMs) specified by large volume fractions occupied by these interfaces. For instance, following experimental data [7–9], computer simulations [10] and theoretical models [11,12], cracks in mechanically loaded nanocrystalline ceramics and metals often nucleate at and grow along interfaces. During plastic deformation, grain boundaries (GBs) in NCMs serve as sources of partial lattice dislocations and twins [13–18] and effectively conduct such deformation modes as GB sliding [19–21], Coble creep [22,23], triple junction diffusional creep [24] and rotational deformation [25–29]. Furthermore, recent experimental observations [30–45] and computer simulations [46–48] have indicated that GB migration and grain growth processes intensively occur in mechanically loaded ultrafine-grained materials and NCMs. For instance, Gianola et al. [39] observed room temperature grain growth in nanocrystalline Al films in the course of their plastic deformation at quite high levels of applied stress. The yield stress was in the range 91–116 MPa, and the ultimate tensile strength was in the range 149–190 MPa [39]. These values are much larger than those (<50 MPa) characterizing plastic deformation in conventional coarse-grained polycrystalline Al. Furthermore, Gianola et al. [39] observed significant grain growth only in highly stressed regions, including the areas near the tips of slowly growing cracks. On the basis of their experimental data, Gianola et al. [39] concluded that grain growth occurs through the stress-induced GB migration at high local stresses. Farkas et al. [48] reported simulation results showing GB motion in nanocrystalline Ni with an ultrasmall grain size of 5 nm. In their molecular dynamics and

* Corresponding author. Tel.: +7 812 321 4764; fax: +7 812 321 4771.
E-mail address: ovidko@def.ipme.ru (I.A. Ovid'ko).

1359-6454/$34.00
doi:10.1016/j.actamat.2008.02.004

empirical potential simulations at room temperature, plastic flow and associated GB motion occurred at a high stress level of 2.5 GPa. These simulations indicate that high applied stresses are needed to initiate GB migration in NCMs. Farkas et al. [48] observed GB mobility for distances up to 2.5 nm, or half the grain size.

Stress-driven GB migration is treated as a special deformation mechanism operating in NCMs (for a detailed discussion, see review article Ref. [5]). A very similar process of stress-driven GB migration occurs in bicrystals [49–54]. In doing so, the stress-driven migration of a GB in a bicrystal is coupled to shear deformation of the crystal lattice traversed by the migrating GB. For instance, GB migration coupled to shear in Al bicrystals has been observed in experiments [53,54]. In these experiments, the applied stresses were quite small (<1 MPa). The theory of the stress-driven GB migration coupled to shear deformation in bicrystals was developed by Cahn et al. [50–52]. Its basic statements are in good agreement with both experimental data [53,54] and the results of computer simulations [51,52,55,56] of the migration of low- and high-angle symmetric tilt boundaries in bicrystals. In addition, the coupling of GB migration and shear has been confirmed by computer simulations [57] of GB sliding through the motion of GB dislocations in a Fe bicrystal. In these simulations, the glide of dislocations has been shown to result in coupled motion of the boundary in directions parallel and perpendicular to itself.

Stress-driven GB migration processes coupled to shear in bicrystals are different from those in NCMs and coarse-grained polycrystals due to the difference in their geometric features (e.g. [58,59]). The shear coupled to GB migration in a bicrystal is easily accommodated by a change of the bicrystal shape, in which case the stress needed to initiate the migration process is low. At the same time, the crystal region where the shear coupled to GB migration occurs in a nanocrystalline solid commonly represents an internal region in the solid, and the shear is strongly hampered by the surrounding material. In Ref. [58], the stress-induced GB migration in a nanoscale grain of a nanocrystalline metal was briefly described as a special deformation mode accommodated by the formation of wedge disclinations (rotational defects creating internal elastic strains and stresses). It was theoretically shown that, if shear coupled to migration of a GB occurs in a NCM, it produces a quadrupole of wedge disclinations at the edges of the region traversed by the migrating GB [58].

The presence of disclinations and other defects serving as internal stress sources in NCMs crucially influences their fracture behavior (for a review, see Ref. [60]). In this context, of particular interest are the effects of the stress-driven GB migration and associated formation of disclinations on fracture processes in NCMs. The main aim of this paper is to suggest theoretical models that describe the effects of GB migration (coupled to shear and formation of disclinations) on both the formation of nanocracks (Section 4) and growth of pre-existing, comparatively large cracks (Section 5) in deformed nanocrystalline ceramics and metals. These theoretical models are based on the results of both the geometric consideration of the stress-driven GB migration in NCMs (Section 2) and the brief analysis of the brittle fracture behavior exhibited by nanocrystalline metals with the finest grains (Section 3).

2. Geometry of stress-driven migration of GBs in NCMs

The geometric features of the stress-driven GB migration are very important for understanding its effects on fracture processes in NCMs. In Ref. [58], the GB migration geometry in NCMs was briefly discussed. In this section, we consider in detail the geometry of stress-driven GB migration (coupled to shear and accommodated by the formation of disclinations) in NCMs and compare it with the geometry of such a migration process in bicrystals. Following Refs. [50–52], the stress-driven migration of a GB in a bicrystal is coupled to shear deformation of the crystal lattice traversed by the migrating GB and results in a change of the bicrystal shape (Fig. 1). In the framework of the theory [50–52], the ideal coupling (in the absence of GB sliding) is described by the linear relationship $v_{\|} = \beta v_n$, where $v_{\|}$ and v_n are the velocities of the relative grain translation and normal GB motion, respectively, and β is the coupling factor. In face-centered cubic (fcc) crystals, for symmetric tilt boundaries with misorientation angles ranging from 0° to 90°, there is a positive and a negative branch of coupling, at which the coupling factor β is positive and negative, respectively [50–52]. For instance, [0 0 1] symmetric tilt GBs in copper show positive coupling if the GB tilt angle ranges from 0° to approximately 35°, and negative coupling if the GB tilt angle ranges from approximately 35° to 90° [52]. The coupling factor is related to the GB tilt misorientation ω as follows [51,52]: $\beta \approx 2\tan(\omega/2)$ and $\beta \approx -2\tan(\pi/4 - \omega/2)$ in the positive and negative branches of coupling, respectively.

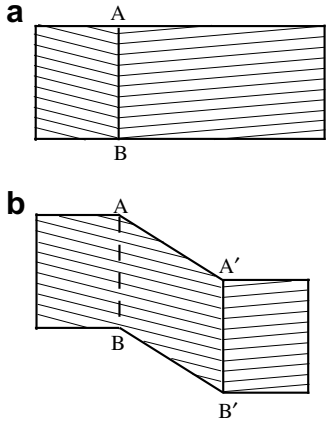

Fig. 1. Stress-driven migration of a tilt boundary in a deformed bicrystal. (a) and (b) depicts the initial and final state, respectively. The boundary migration results in a shear of the area traversed by this boundary. The shear is accommodated by a change in the bicrystal shape.

In light of the standard representation of low-angle tilt GBs as walls of lattice dislocations [61], migration of a low-angle boundary is described as the stress-driven motion of the lattice dislocations that form this boundary [51,52]. In the framework of the dislocation theory of GBs, high-angle GBs are effectively described as those containing continuously distributed GB dislocations [61–63]. In this context, migration of a high-angle tilt GB is represented as the stress-driven motion of the GB dislocations that form the GB [51,52]. Within the dislocation model, the critical stress for GB migration in a bicrystal is the lowest stress needed to initiate dislocation motion. In particular, for migration of a low-angle lilt GB at low temperatures, the critical stress is the Peierls–Nabarro stress causing glide of lattice edge dislocations [51,52]. Since the Peierls–Nabarro stress is low in fcc metals [64], migration of low-angle tilt GBs can occur at low applied stresses. This view is confirmed by experiments [53,54] showing migration of low-angle tilt GBs in Al bicrystals at low applied stresses <1 MPa.

The shear coupled to GB migration in a nanocrystalline specimen is strongly hampered by surrounding nanoscale grains (Fig. 2), in contrast to the situation with a bicrystal in which shear coupled to GB migration is freely accommodated by a change in the bicrystal shape (Fig. 1). Let us consider the geometry of the stress-induced GB migration and its accommodation in NCMs. In doing so, in order to simplify our analysis, we consider a two-dimensional model arrangement of nanoscale grains with pure tilt GBs, including a vertical GB that migrates in a rectangular grain as shown in Fig. 3. (Such a rectangular grain serves as a good model of elongated grains formed in nanocrystalline specimens at superplastic deformation; see e.g. Ref. [43].) The tilt GBs are either low- or high-angle boundaries containing discrete or continuously distributed dislocations as schematically shown in Fig. 3. In particular, the vertical GB contains a finite wall-like ensemble of dislocations that provide its tilt misorientation ω. In its initial state, the vertical GB (Fig. 3a) terminates at the GB junctions A and B, which are supposed to be geometrically compensated. There are no angle gaps at these triple junctions or, in other words, the sum of tilt misorientation angles of all GBs joining at each of these junctions is equal to zero, where summation of the angles is performed clockwise along a circuit surrounding a triple junction (for details, see Refs. [65,66]). In the case under consideration, the following balance equations are valid:

$$\theta_1 + \theta_2 + \omega = 0 \quad \text{(for GB junction A)}, \tag{1}$$

$$\theta_3 + \theta_4 - \omega = 0 \quad \text{(for GB junction B)}. \tag{2}$$

Following the geometric theory of triple junctions [65,66], the geometrically compensated GB junctions A and B (Fig. 3a) do not create long-range stresses.

Let us consider the situation where the vertical GB migrates from the position AB to the position A′B′ (Fig. 3b), and no other accommodating structural transformations occur. As a result of the migration, the angle gaps

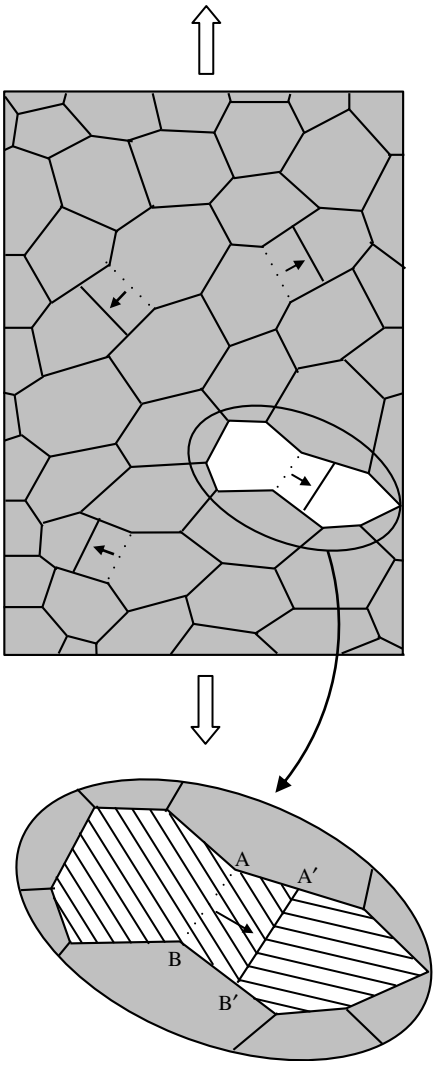

Fig. 2. Stress-driven migration of grain boundaries in a deformed nanocrystalline specimen. The shear coupled to migration is hampered by surrounding grains. The magnified inset highlights the geometry of a nanograin group hampering shear coupled to grain boundary migration.

$-\omega$ and ω appear at the GB junctions A and B, respectively (Fig. 3b). That is, the sum of the misorientation angles at junction A after GB migration is $\theta_1 + \theta_2$, which is equal to $-\omega$ according to formula (1). The sum of the misorientation angles at junction B after GB migration is $\theta_3 + \theta_4$, which is equal to ω according to formula (2). In addition, GB migration results in formation of two new triple junctions A′ and B′ characterized by the angle gaps ω and $-\omega$, respectively. That is, the sum of the misorientation angles at junction A′ is equal to ω, as can be seen directly in Fig. 3b. The sum of the misorientation angles at the junction B′ is equal to $-\omega$ (Fig. 3b).

Within the theory of defects in solids, the GB junctions A, B, A′ and B′ characterized by the angle gaps $\pm\omega$ are defined as partial wedge disclinations (rotational defects) that serve as powerful stress sources characterized by the disclination strengths $\pm\omega$ [5,65–69]. The disclinations at the points A, B, A′ and B′ form a quadrupole configuration

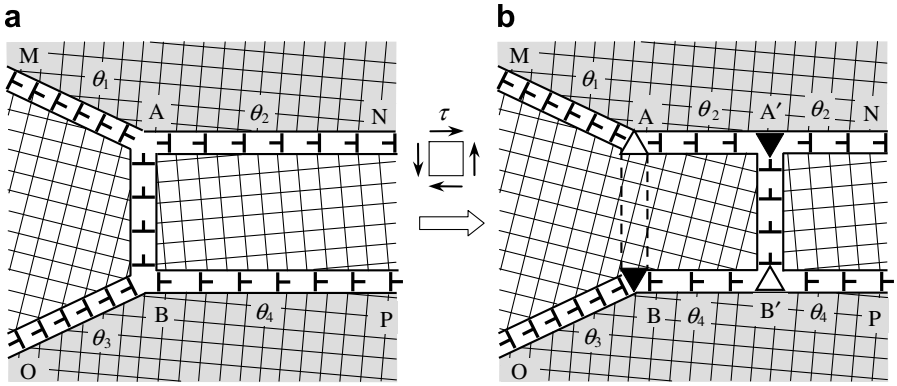

Fig. 3. Stress-induced migration of a tilt boundary in a nanocrystalline specimen (two-dimensional model). The vertical tilt boundary migrates from its initial position AB (a) to the final position A′B′ (b). The shear coupled to migration is accommodated by formation of disclinations (triangles) at grain boundary junctions A, A′, B and B′.

whose formation accommodates GB migration coupled to shear in a nanocrystalline specimen. The disclination quadrupole creates internal stresses screened at distances that are around the largest size (largest interspacing between the disclinations) of the quadrupole.

In terms of the dislocation approach used in the theory of GB migration coupled to shear in bicrystals [50–52], formation of wedge disclinations during GB migration is interpreted as follows. Once again, let us consider the situation where the vertical tilt GB migrates (Figs. 3 and 4), and no other accommodating structural transformations occur. The vertical GB with a tilt misorientation ω and finite length contains a finite wall of either discrete dislocations, if the GB is a low-angle tilt boundary, or continuously distributed dislocations, if the GB is a high-angle tilt boundary. For definiteness, let us consider migration of the vertical high-angle tilt boundary (in the positive branch of coupling) from its initial position AB to the final position A′B′ in a nanocrystalline specimen and its continuum model (Fig. 4). The migration of the vertical tilt GB is equivalent to the formation of two finite dislocation walls, AB and A′B′, that consist of continuously distributed dislocations with opposite Burgers vectors as shown in Fig. 4a–d. Within the theory of defects in solids, the finite dislocation walls serve as stress sources that are disclinations characterized by strengths $\pm\omega$ and located at the ends of the dislocation walls [5,68,69] (Fig. 4e and f). The disclinations compose a quadrupole whose formation accommodates GB migration coupled to shear in a nanocrystalline specimen (Fig. 4e and f).

Thus, the shear that accompanies GB migration in a nanocrystalline specimen is hampered by the surrounding grains (Fig. 2). The shear is effectively accommodated by formation of a wedge disclination quadrupole (Figs. 3 and 4), creating elastic strains. In these circumstances, the energy associated with the formation of the disclination quadrupole comprises the main contribution to the critical shear stress τ_{cr} for GB migration in a nanocrystalline specimen. Following Ref. [58], the critical stress τ_{cr} for the start of migration of a tilt GB with misorientation ω in a nanograin of size d is given as:

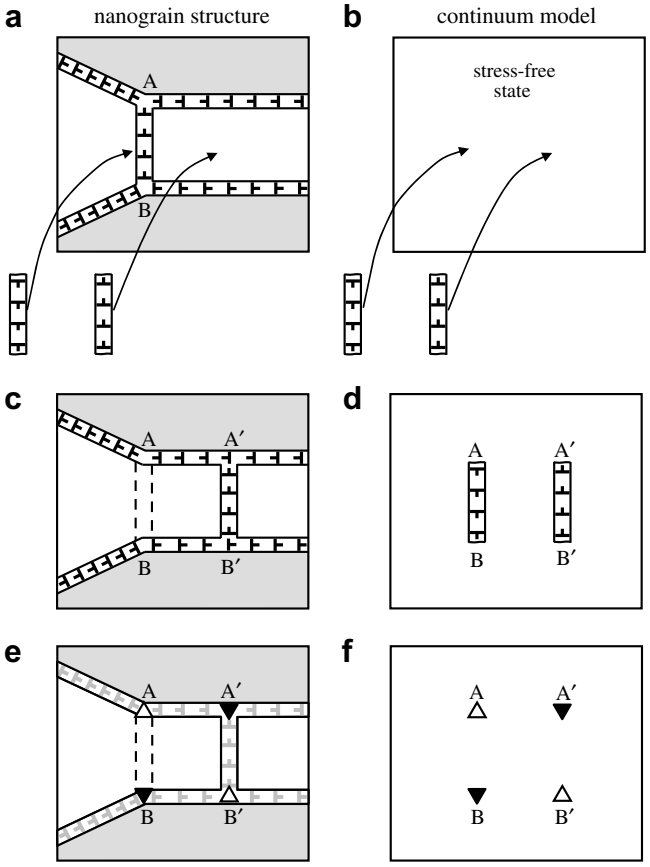

Fig. 4. Migration of a high-angle tilt boundary represented as a finite wall of continuously distributed dislocations. Description in terms of the nanograin structure ((a), (c) and (e)) and its continuum model ((b), (d) and (f)) are presented. (a) and (b) Initial, stress-free state. (c) and (d) Final state of a nanocrystalline specimen, after migration of the vertical tilt boundary from its initial position AB to the final position A′B′. The final state can be obtained by addition of two dislocation walls to the initial state. These walls are the finite wall AB of dislocations having Burgers vectors opposite to those composing the tilt boundary in its initial position, and the finite wall A′B′ of dislocations identical to those composing the tilt boundary in its final position. (e) and (f) The finite dislocation walls AB and A′B′ as stress sources are equivalent to wedge disclinations (triangles) characterized by strengths $\pm\omega$ and located at the end points A, A′, B and B′ of the dislocation walls.

$$\tau_{cr} \approx \frac{G\omega}{2\pi(1-\nu)} \frac{s}{d} \ln(d/s), \quad s < d, \tag{3}$$

where G denotes the shear modulus, ν is the Poisson's ratio and s is the path moved by the migrating GB at the beginning of its migration. (s is around several crystal lattice parameters.) Dao et al. [5] noted that when the tilt misorientation of a migrating GB is in the range 5–30° and the grain size is in the range 5–30 nm, the model [58] gives values of the critical stress τ_{cr} (see formula (3)) in the range 20–300 MPa, well in the prevailing range of stress levels for many nanocrystalline fcc metals with grain sizes in that range.

Furthermore, it is important to note that the critical stress τ_{cr} given by formula (3) is commonly much larger than the Peierls–Nabarro stress. This reflects the experimentally detected fact that the critical stress necessary to initiate GB migration and grain growth in NCMs is much larger than that in bicrystals. For instance, in the case of experimentally observed GB migration in deformed nanocrystalline Al films [39], the yield stress ranges from 91 to 116 MPa, and the ultimate tensile strength ranges from 149 to 190 MPa. These values are by several orders larger than those (<1 MPa) for stress-driven GB migration in Al bicrystals [53,54]. In the light of our geometric analysis of GB migration in NCMs, the difference in the critical stress level (for GB migration start) between bicrystals and NCMs is naturally attributed to the difference in accommodation mechanisms. The shear coupled to GB migration in a bicrystal and nanocrystalline specimen is freely accommodated by a change in the bicrystal shape (Fig. 1) and strongly hampered by surrounding nanoscale grains (Fig. 2), respectively.

Finally, note that along with the formation of a disclination quadrupole, alternative accommodating mechanisms can come into play. For instance, such mechanisms accommodating stress-driven GB migration can be (i) diffusion; (ii) emission of lattice dislocations from the GB segments AA′ and BB′; and (iii) migration of these GB segments under the same applied stress as well as under the back-stresses produced by the disclinations. Furthermore, in general, migration of the vertical GB can lead to changes in the energies and other characteristics of the GB segments AA′ and BB′, and the tension of the above GB segments can either promote or retard the migration of the vertical GB. In addition, segregation of impurities at GBs can retard or even completely suppress GB migration [32,70]. Consideration of all these additional factors capable of influencing GB migration coupled to shear in NCMs represents a very cumbersome problem whose analysis is beyond the scope of this paper. In the rest of this paper, we will focus our examination on the role of disclinations accommodating GB migration in fracture processes in NCMs.

3. Ductile-to-brittle transition in nanocrystalline metals

In general, stress-driven GB migration accompanied by the formation of disclinations is capable of strongly influencing fracture processes in nanocrystalline ceramics and metals. However, GB migration is expected to be most pronounced in metallic materials, most of which are commonly considered to be ductile. At the same time, in ductile materials, crack growth is effectively suppressed by dislocation emission from crack tips, thus making the effects of GB migration on fracture not very important. Recently, however, it has been experimentally demonstrated that nanocrystalline metallic materials tend to become brittle when their grain size becomes smaller than some critical size [8,71–73]. For example, Li and Ebrahimi [8,72] documented brittle intergranular fracture of plastically deformed nanocrystalline Ni–15% Fe alloy with a grain size of 9 nm. The behavior of this Ni–15% Fe alloy was in contrast to the ductile failure behavior of pure Ni with a larger grain size of 44 nm, which fractured only after significant reduction in area (necking) [8,72]. Gan and Zhou [71] observed intergranular cracking of deformed nanocrystalline Fe alloys and a nearly two-fold decrease in fracture toughness (characterizing the resistance to crack propagation) with the reduction in grain size from 35 to 11 nm. A brittle fracture morphology was also observed in cyclically deformed nanocrystalline Ni with a 40 nm grain size [73].

The ductile-to-brittle transition in nanocrystalline metallic materials at a critical grain size has been attributed to the very limited dislocation activity in NCMs with the finest grains [8,72] although the exact mechanisms for this transition have not yet been identified. In our opinion, this transition can be related to the role of GBs as barriers for dislocation motion. Indeed, a solid is intrinsically ductile if it has a high resistance to crack propagation. It is generally accepted that crack growth in ductile materials is retarded through dislocation emission from crack tips [74–76] resulting in crack blunting (e.g. [76–78]). It is therefore assumed that a solid is ductile if conditions favor a crack emitting a dislocation rather than advancing [74,75,77]. However, in the case of NCMs, GBs hinder the emitted dislocations from moving far away from the crack tip (Fig. 5). As a

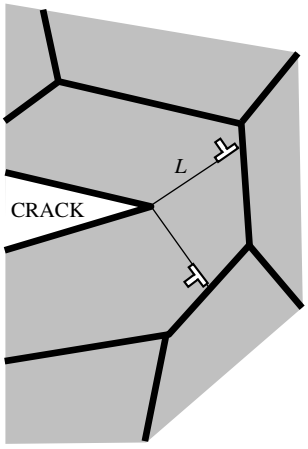

Fig. 5. Dislocation emission from a crack tip in a nanocrystalline material. Emitted dislocations stop at the nearest grain boundaries. The ledges at the crack tip created due to dislocation emission are not shown.

result, in NCMs the previously emitted dislocations strongly repulse newly emitted dislocations and can stop the emission of subsequent dislocations. The repulsion increases with decreasing distance L between the crack tip and the dislocation previously emitted and stopped at the nearest GB (Fig. 5). Therefore, the suppression of dislocation emission from a crack tip by previously emitted dislocations is enhanced with decreasing grain size d in the material containing the crack. (Note that the emitted dislocations also exert a shielding effect on the crack tip [76,77,79,80], i.e. hinder crack growth. A detailed study of the competition between the two effects is in progress. The initial results show that the suppression of dislocation emission from a crack tip by previously emitted dislocations is generally stronger that their hindering effect on crack propagation.) In these circumstances, the discussed suppression of dislocation emission from the crack tip can cause the experimentally detected [8,71–73] brittle fracture of nanocrystalline metals with the finest grains.

Thus, following experimental data [8,71–73], nanocrystalline metallic materials with the finest grains tend to show the brittle fracture behavior. The experiments in question allow us to consider the role of GB migration in fracture processes in nanocrystalline metals with the finest grains, treating these materials as brittle ones. In doing so, in the next sections, which are focused on the analysis of the formation of nanocracks and growth of comparatively large cracks in the presence of GB migration in nanocrystalline metals with the finest grains and nanoceramics, we will use the formulas of the theory of brittle fracture and treat GB migration as a toughening mechanism that can slow down the growth of large cracks.

4. Nanocrack generation at a disclination dipole

As shown in Section 2, stress-driven GB migration leads to the formation of GB disclinations creating high local stresses. These stresses are capable of inducing the nucleation of nanocracks. In this section, we suggest a theoretical model describing nanocrack nucleation accompanying GB migration.

Let us consider a deformed nanocrystalline specimen – either metallic or ceramic solid with nanocrystalline structure – where GB migration occurs under the action of a shear stress τ. Following Ref. [58] and Section 2 of this paper, the migration of a GB with the tilt misorientation ω gives rise to the formation of a quadrupole of wedge disclinations with strengths $-\omega$ and ω (see Figs. 3 and 4). At the beginning of the GB migration process, the length s of GB migration is generally significantly smaller than the GB length. In these circumstances, the disclination quadrupole consists of two disclination dipoles whose stress fields are screened at a distance of the order of s. As a corollary, the stress field of one disclination dipole does not affect nanocrack nucleation in the vicinity of the other dipole and vice versa. Therefore, to a first approximation, in considering the conditions for the formation of a nanocrack generated at one of the quadrupole disclinations, it is sufficient to take into account only the applied stress and the stress field of one of the two disclination dipoles that compose the disclination quadrupole. The stress field of the other disclination dipole is neglected.

Thus, in order to determine the conditions of nanocrack nucleation at the beginning of the GB migration process, we consider a dipole of wedge disclinations (Fig. 6), a part of the disclination quadrupole produced due to GB migration. The geometry of the dipole of wedge disclinations is adequately described in the Cartesian coordinate system (x, y) shown in Fig. 6. In this coordinate system, the disclinations with strengths ω and $-\omega$ lie on the x-axis at points $x = -s$ and 0, respectively. The points bound the horizontal GB segment whose tension and possible migration are neglected in our model.

Let the stress field of the disclination dipole and the applied stress τ induce the formation of a flat nanocrack of length l. The nanocrack is assumed to nucleate at the disclination with strength $-\omega$, along a GB in the region where the tensile stresses exerted on the crack surfaces by the disclination dipole are highest (see Fig. 6).

To estimate the conditions for nanocrack formation, we will use the energetic criterion of crack growth [81]:

$$F > 2\gamma_e, \tag{4}$$

where F is the energy release rate, $\gamma_e = \gamma - \gamma_b/2$, γ is the specific surface energy and γ_b is the energy of a GB per unit area of the GB. The term γ_b appears in formula (4) because the formation of a nanocrack growing along a GB releases the extra energy of the GB [11,12]. The nanocrystalline specimen is assumed to be an elastically isotropic solid with shear modulus G and Poisson ratio ν. In the considered case of an elastically isotropic solid and plane strain state, the energy release rate F is given as [81]:

$$F = \frac{\pi(1-\nu)l}{4G}\left(\bar{\sigma}_{yy}^2 + \bar{\sigma}_{xy}^2\right), \tag{5}$$

where $\bar{\sigma}_{yy}$ and $\bar{\sigma}_{xy}$ are the mean weighted values of the stresses σ_{yy} and σ_{xy} created by the applied stress τ and disclination dipole. The mean weighted stresses $\bar{\sigma}_{yy}$ and $\bar{\sigma}_{xy}$ are defined as [81]

$$\bar{\sigma}_{my} = \frac{2}{\pi l}\int_0^l \sigma_{my}(x, y=0)\sqrt{\frac{x}{l-x}}\,dx, \quad m = x, y. \tag{6}$$

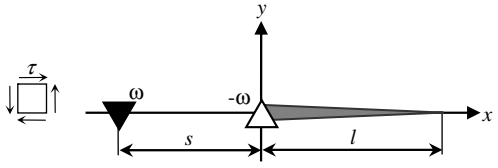

Fig. 6. Formation of a nanocrack at a disclination dipole in a plastically deformed solid.

The stresses $\sigma_{xy}(x, y = 0)$ and $\sigma_{yy}(x, y = 0)$ are given as follows [68]: $\sigma_{xy}(x, y = 0) = \tau$, $\sigma_{yy}(x, y = 0) = D\omega \ln|(x+s)/x|$, where $D = G/[2\pi(1-\nu)]$. Substitution of the latter relations for the stresses σ_{xy} and σ_{yy} as well as formulae (5) and (6) to formula (4), yields the following condition of energetically favorable crack growth: $q(\tilde{l}) > q_c$, where $\tilde{l} = l/s$,

$$q(\tilde{l}) = \tilde{l}\left[\left(\frac{2\left(\sqrt{1+\tilde{l}}-1\right)}{\tilde{l}} - \ln\frac{\sqrt{1+\tilde{l}}+1}{\sqrt{1+\tilde{l}}-1}\right)^2 + \left(\frac{\tau}{D\omega}\right)^2\right], \tag{7}$$

and $q_c = 16\pi(1-\nu)(2\gamma - \gamma_b)/(Gs\omega^2)$.

The dependence $q(\tilde{l})$ is shown in Fig. 7, for $\tau = 1$ GPa, $\omega = \pi/6$, and the parameters G and ν for Ni [82] ($G = 79$ GPa and $\nu = 0.31$). The horizontal lines in Fig. 7 show the values of q_c for the case of nanocrystalline Ni (with $\gamma = 1.725$ J m^{-2} and $\gamma_b = 0.69$ J m^{-2} [64]), $\omega = \pi/6$ and different values of the dipole arm s ($s = 6$ and 4 nm for the solid and dashed horizontal line, respectively). It follows from Fig. 7 that $q(\tilde{l})$ first increases and then decreases with rising $\tilde{l}$. In the situation where the values of the disclination strength ω (equal to the GB misorientation angle) and/or the distance s between the disclinations are not too large, we have: $q(\tilde{l}) < q_c$, for any nanocrack length in the nanocrack length range shown in Fig. 7 (see the dashed horizontal line in Fig. 7). In this situation, the formation of a nanocrack is not likely. In contrast, for large enough values of ω and/or s, nanocrack growth is energetically favored in a nanocrack length interval $l_{e1} < l < l_{e2}$. In this case, the critical lengths l_{e1} and l_{e2} are determined by the points of intersection of the curve $q(\tilde{l})$ with the solid horizontal line that shows the value of q_c. Nanocrack nucleation and growth in the range $l < l_{e1}$ requires thermal fluctuations. Its subsequent growth within the length range $l_{e1} < l < l_{e2}$ occurs athermally. Further nanocrack growth is energetically forbidden. For the parameter values used in the plot in Fig. 7 and $s = 6$ nm, we have: $l_{e1} \approx 0.1s = 0.6$ nm and $l_{e2} \approx 1.8s = 10.8$ nm. Thus, disclination dipoles formed due to GB migration can induce the formation of sufficiently large nanocracks.

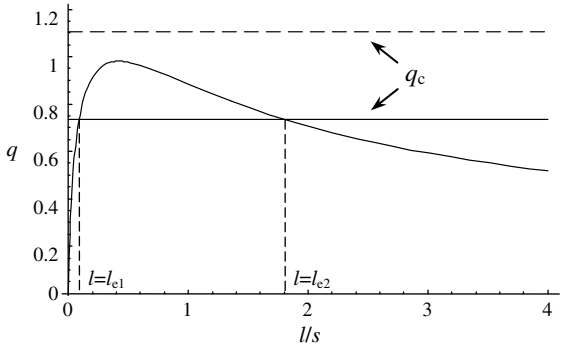

Fig. 7. Dependence of the parameter q on the normalized nanocrack length l/s. The solid and dashed horizontal lines show the values of the parameter q_c for the cases $s = 6$ and 4 nm, respectively.

Besides the applied stress level, material parameters (in particular, the ratio of its effective surface energy to the shear modulus) strongly affect the possibility for the formation of nanocracks as a result of GB migration. For example, for nanocrystalline α-Al_2O_3 (with the following typical parameter values [83,84]: $G = 169$ GPa, $\nu = 0.23$, $\gamma = 1.69$ J m^{-2}), we obtain for $\tau = 3$ GPa, $\omega = \pi/6$ and the exemplary case of $\gamma_b = 0.5\gamma$ that nanocracks can nucleate in both cases $s = 4$ and 6 nm and are characterized by the equilibrium lengths $l_{e2} \approx 10$ and 33 nm for $s = 4$ and 6 nm, respectively. In contrast, in the case of pure nanocrystalline Al (with the following typical parameter values [64,82]: $G = 27$ GPa, $\nu = 0.34$, $\gamma = 1.2$ J m^{-2} and $\gamma_b = 0.5$ J m^{-2}), for $\tau = 1$ GPa and $\omega = \pi/6$, nanocracks are not generated at $s = 4$ and 6 nm and start to nucleate only if $s > 8.4$ nm.

5. Effect of grain boundary migration on crack growth

Besides the initiation of nanocrack nucleation, the growth of pre-existing, comparatively large cracks is affected by stress-induced GB migration. In this section, we consider the influence of GB migration on crack growth and the critical crack length beyond which GB migration is favored to advance.

Let us consider a nanocrystalline specimen – either metallic or ceramic solid with nanocrystalline structure – containing a straight crack of length L. For illustration, we consider pure mode I loading, wherein the symmetry of the applied load is such that the crack faces tend to open rather than shear against one another. The loading is characterized by the uniaxial tensile remote load σ_0 applied perpendicular to the crack surface (see Fig. 8).

When a mechanical load is applied to the specimen, the stress concentration near the crack tip can drive the migration of GBs in its vicinity. GB migration partly relieves high strain energy accumulated near the crack tip and

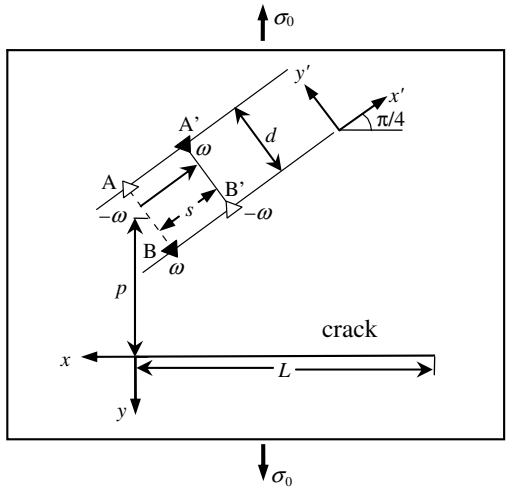

Fig. 8. Geometry of a crack that propagates near a migrating grain boundary. Stress-induced grain boundary migration is realized through the formation of a quadrupole of wedge disclinations and consequent movement of a dipole of disclinations.

can thereby slow down crack propagation. This effect of GB migration is quantitatively characterized by an increase in the critical crack length (above which crack advance becomes energetically favorable). In order to examine the effect of GB migration on crack propagation, we consider a nanocrystalline solid with a model arrangement of rectangular grains divided by GBs. Let a straight crack of length L terminate at a distance p from the middle of a GB AB (Fig. 8). We introduce Cartesian coordinate systems (x, y) and (x', y') as shown in Fig. 8. Due to the action of an external tensile stress σ_0 (applied as shown in Fig. 8 and creating the shear stress $\tau = \tau_{x'y'} = \sigma_0/2$ acting on the migrating GB) and its stress concentration caused by the crack, the GB AB migrates to a new position A′B′ (Fig. 8).

As has been discussed above, the migration of a tilt GB leads to the formation of a quadrupole of wedge disclinations with strengths $\pm\omega$, equal in magnitude to the misorientation angle of the migrating GB. We denote the length of the GB AB as d, and its migration distance AA′ as s. In addition, these distances serve as characteristic scales (called "arms") of the disclination quadrupole. In order to estimate, to a first approximation, the effect of GB migration on crack propagation, we assume that the crack plane makes the angle $\pi/4$ with the x'-axis and the angle $\pi/2$ with the vector $\boldsymbol{p}$ directed from the crack tip to the middle of the GB AB (see Fig. 8). Thus, we choose the crack location at which propagation is easiest. The above assumptions simplify our mathematical analysis, and at the same time do not mask the key aspects of the problem.

To estimate the effect of GB migration on crack propagation, we will use energetic criterion (4), where we put $\gamma_e = \gamma$, for a crack growing in a grain interior, and $\gamma_e = \gamma - \gamma_b/2$, for a crack growing along a GB. As in Section 4, we model the solid as an infinite isotropic medium. For the calculation of the energy release rate F, we calculate the total stresses σ^q_{xy} and σ^q_{yy} created in the crack plane by the disclination quadrupole and external stress σ_0. Then, using the calculation scheme similar to that employed in the previous section, we obtain the following condition of the energetically favorable crack growth: $Q > Q_c$, where

$$Q = \frac{1}{Ld}\left[\left(K + \omega\int_0^L g_{yy}(-x)\sqrt{\frac{L-x}{x}}\,dx\right)^2 + \left(\omega\int_0^L g_{xy}(-x)\sqrt{\frac{L-x}{x}}\,dx\right)^2\right], \tag{8}$$

$$g_{yy}(x) = \frac{1}{2}\ln\frac{[(x+x_1)^2+(p-x_1)^2][(x+x_{2-})^2+(p+x_{2+})^2]}{[(x-x_1)^2+(p+x_1)^2][(x+x_{2+})^2+(p+x_{2-})^2]} - \frac{(p-x_1)^2}{(x+x_1)^2+(p-x_1)^2} + \frac{(p+x_1)^2}{(x-x_1)^2+(p+x_1)^2} - \frac{(p+x_{2+})^2}{(x+x_{2-})^2+(p+x_{2+})^2} + \frac{(p+x_{2-})^2}{(x+x_{2+})^2+(p+x_{2-})^2}, \tag{9}$$

$$g_{xy}(x) = \frac{(x+x_1)(p-x_1)}{(x+x_1)^2+(p-x_1)^2} - \frac{(x-x_1)(p+x_1)}{(x-x_1)^2+(p+x_1)^2} + \frac{(x+x_{2-})(p-x_{2+})}{(x+x_{2-})^2+(p-x_{2+})^2} + \frac{(x+x_{2+})(p-x_{2-})}{(x+x_{2+})^2+(p-x_{2-})^2}, \tag{10}$$

$x_1 = d/(2\sqrt{2})$, $x_{2\pm} = s/\sqrt{2} \pm x_1$, $K = \sigma_0\pi^2(1-\nu)L/G$, and $Q_c = 8\pi^3(1-\nu)\gamma_e/(Gd)$.

The condition $Q = Q_c(L = L_e)$ gives the critical crack length L_e at which its growth becomes energetically favorable. Let us estimate the effect of GB migration on the critical crack length for the case of nanocrystalline Ni. Let us put $\sigma_0 = 1$ GPa, $\omega = 5°$, $d = 15$ nm, $s = 5$ nm and $p = d/2$. Then from formulas (8)–(10) and the relation $Q = Q_c(L = L_e)$ we find: $L_e = 663$ nm, for a crack growing in a grain interior, and $L_e = 547$ nm, for a crack growing along a GB. At the same time, in the absence of GB migration (the case of $\omega = 0$), we have: $L_e = 503$ nm, for a crack growing in a grain interior, and $L_e = 402$ nm, for a GB crack. Thus, GB migration in nanocrystalline Ni can increase the critical crack length (beyond which its athermal growth is energetically beneficial).

6. Concluding remarks

We have theoretically described the geometric features of stress-driven GB migration and its effects on both the formation of nanocracks and growth of comparatively large cracks in deformed nanocrystalline ceramics and metals. It has been found that the shear coupled to GB migration in a nanocrystalline specimen is strongly hampered by surrounding nanoscale grains (Fig. 2) and can be effectively accommodated by formation of wedge disclination quadrupoles. With this accommodation mechanism, a high level of critical stresses is needed to initiate GB migration in NCMs (in contrast to the situation with a bicrystal where shear coupled to GB migration is freely accommodated by a change in the bicrystal shape (Fig. 1) and thereby occurs at low applied stresses). The disclinations, whose formation accommodates the GB migration, create high local stresses capable of initiating the formation of nanocracks in NCMs. We have theoretically described the conditions at which the formation of nanocracks is energetically favorable and calculated the critical lengths, l_{e1} and l_{e2} of such nanocracks.

Furthermore, in this paper, the stress-driven migration of GBs is shown to relieve local stresses near the tips of comparatively large cracks in brittle nanocrystalline metals with the finest grains and nanoceramics. It has been found that GB migration in these materials can increase the critical crack length (beyond which its athermal propagation is energetically beneficial). In this context, the stress-driven migration of GBs can serve as a special toughening mechanism in nanocrystalline ceramics and metals with the finest grains. Its effective action in NCMs is due to the

following two factors: (i) NCMs are characterized by large volume fractions occupied by GBs; and (ii) plastic deformation occurs at very high stresses in these materials. At the same time, the stress-driven migration of GBs hardly contributes to toughening of coarse-grained polycrystalline metals where toughening mechanisms associated with plastic flow are realized through conventional dislocation emission from crack tips (e.g. [76–78]).

Acknowledgements

This work was supported, in part, by the Aristotle University of Thessaloniki (Subcontract of the Contract HPRN-CT-2002-00198), the Office of US Naval Research (Grant No. 00014-07-1-0295), Russian Federal Agency of Science and Innovations (Contract 02.513.11.3190 of the Program "Industry of Nanosystems and Materials"), the National Science Foundation Grant CMMI #0700272, Russian Academy of Sciences Program "Structural Mechanics of Materials and Construction Elements", and the St. Petersburg Center of the Russian Academy of Sciences.

References

[1] Kumar KS, Suresh S, Swygenhoven H. Acta Mater 2003;51:5743.
[2] Wolf D, Yamakov V, Phillpot SR, Mukherjee AK, Gleiter H. Acta Mater 2005;53:1.
[3] Han BQ, Lavernia E, Mohamed FA. Rev Adv Mater Sci 2005;9:1.
[4] Meyers MA, Mishra A, Benson DJ. Prog Mater Sci 2006;51:427.
[5] Dao M, Lu L, Asaro RJ, De Hosson JTM, Ma E. Acta Mater 2007;55:4041.
[6] Gutkin MYu, Ovid'ko IA. Plastic deformation in nanocrystalline materials. Berlin: Springer; 2004.
[7] Kumar KS, Suresh S, Chisholm MF, Horton JA, Wang P. Acta Mater 2003;51:387.
[8] Li H, Ebrahimi F. Appl Phys Lett 2004;84:4307.
[9] Zhan G-D, Kuntz JD, Wan J, Mukherjee AK. Nat Mater 2003;2:38.
[10] Farkas D, van Petegem S, Derlet PM, van Swygenhoven H. Acta Mater 2005;53:3115.
[11] Ovid'ko IA, Sheinerman AG. Acta Mater 2004;52:1201.
[12] Ovid'ko IA, Sheinerman AG. Acta Mater 2005;53:1347.
[13] Chen M, Ma E, Hemker KJ, Sheng H, Wang Y, Cheng X. Science 2003;300:1275.
[14] Liao XZ, Zhou F, Lavernia EJ, Srinivasan SG, Baskes MI, He DW, et al. Appl Phys Lett 2003;83:632.
[15] Liao XZ, Srinivasan SG, Zhao YH, Baskes MI, Zhu YT, Zhou F, et al. Appl Phys Lett 2004;84:3564.
[16] Zhu YT, Liao XR, Valiev RZ. Appl Phys Lett 2005;86:103112.
[17] Gutkin MYu, Ovid'ko IA, Skiba NV. Phys Rev B 2006;74:172107.
[18] Bobylev SV, Gutkin MYu, Ovid'ko IA. Phys Rev B 2006;73:064102.
[19] Van Vliet K, Tsikata J, Suresh S. Appl Phys Lett 2003;83:1441.
[20] Mukherjee AK. Mater Sci Eng A 2002;322:1.
[21] Gutkin MYu, Ovid'ko IA, Skiba NV. Acta Mater 2004;52:1711.
[22] Masumura RA, Hazzledine PM, Pande CS. Acta Mater 1998;46:4527.
[23] Yamakov V, Wolf D, Phillpot SR, Gleiter H. Acta Mater 2002;50:61.
[24] Fedorov AA, Gutkin MYu, Ovid'ko IA. Scripta Mater 2002;47:51.
[25] Murayama M, Howe JM, Hidaka H, Takaki S. Science 2002;295:2433.
[26] Ovid'ko IA. Science 2002;295:2386.
[27] Gutkin MYu, Ovid'ko IA, Skiba NV. Acta Mater 2003;51:4059.
[28] Shan Zh, Stach EA, Wiezorek JMK, Knapp JA, Follstaedt DM, Mao SX. Science 2004;305:654.
[29] Sergueeva AV, Mukherjee AK. Rev Adv Mater Sci 2006;13:1.
[30] Mukherjee AK. Mater Sci Eng A 2002;322:1.
[31] Jin M, Minor AM, Stach EA, Morris Jr JW. Acta Mater 2004;52:5381.
[32] Soer WA, de Hosson JTM, Minor A, Morris Jr JW, Stach E. Acta Mater 2004;52:5783.
[33] Zhang K, Weertman JR, Eastman JA. Appl Phys Lett 2004;85:5197.
[34] Zhang K, Weertman JR, Eastman JA. Appl Phys Lett 2005;87:061921.
[35] Gai PL, Zhang K, Weertman J. Scripta Mater 2007;56:25.
[36] Liao XZ, Kilmametov AR, Valiev RZ, Gao H, Li X, Mukherjee AK, et al. Appl Phys Lett 2006;88:021909.
[37] Pan D, Nieh TG, Chen MW. Appl Phys Lett 2006;88:161922.
[38] Pan D, Kuwano S, Fujita T, Chen MW. NanoLetters 2007;7:2108.
[39] Gianola DS, Van Petegem S, Legros M, Brandstetter S, Van Swygenhoven H, Hemker KJ. Acta Mater 2006;54:2253.
[40] Gianola DS, Warner DH, Molinari JF, Hemker KJ. Scripta Mater 2006;55:649.
[41] Fan GJ, Fu LF, Choo H, Liaw PK, Browning ND. Acta Mater 2006;54:4781.
[42] Fan GJ, Wang YD, Fu LF, Choo H, Liaw PK, Ren Y, et al. Appl Phys Lett 2006;88:171914.
[43] Xu X, Nishimura T, Hirosaki N, Xie RJ, Yamamoto Y, Tanaka H. Acta Mater 2006;54:255.
[44] De Hosson JTM, Soer WA, Minor AM, Shan Z, Stach EA, Syed Asif SA, et al. J Mater Sci 2006;41:7704.
[45] Soer WA, De Hosson JTM, Minor AM, Shan Z, Syed Asif SA, Warren OL. Appl Phys Lett 2007;90:181924.
[46] Haslam AJ, Moldovan D, Yamakov V, Wolf D, Phillpot SR, Gleiter H. Acta Mater 2003;51:2097.
[47] Sansoz F, Dupont V. Appl Phys Lett 2006;89:111901.
[48] Farkas D, Froseth A, Van Swygenhoven H. Scripta Mater 2006;55:695.
[49] Winning M, Gottstein G, Shvindlerman LS. Acta Mater 2002;50:353.
[50] Cahn JW, Taylor JE. Acta Mater 2004;52:4887.
[51] Cahn JW, Mishin Y, Suzuki A. Philos Mag 2006;86:3965.
[52] Cahn JW, Mishin Y, Suzuki A. Acta Mater 2006;54:4953.
[53] Molodov DA, Ivanov VA, Gottstein G. Acta Mater 2007;55:1843.
[54] Molodov DA, Gorkaya T, Gottstein G. Mater Sci Forum 2007;558–559:927.
[55] Suzuki A, Mishin Y. Mater Sci Forum 2005;502:157.
[56] Mishin Y, Suzuki A, Uberuaga BP, Voter AF. Phys Rev B 2007;75:224101.
[57] Monk J, Hyde B, Farkas D. J Mater Sci 2006;41:7741.
[58] Gutkin MYu, Ovid'ko IA. Appl Phys Lett 2005;87:251916.
[59] Bernstein N. Acta Mater 2008;56.
[60] Ovid'ko IA. J Mater Sci 2007;42:1694.
[61] Sutton AP, Balluffi RW. Interfaces in crystalline materials. Oxford: Clarendon Press; 1995.
[62] Bilby BA. In: Bristol conference report on defects in crystalline materials. London: Physical Society; 1955. p. 123.
[63] Bilby BA. In: Sneddon IN, Hill RP, editors. Progress in solid mechanics, Vol. 1. Amsterdam/New York: North-Holland; 1960. p. 330.
[64] Hirth JP, Lothe J. Theory of dislocations. New York: Wiley; 1982.
[65] Bollmann W. Philos Mag A 1984;49:73.
[66] Bollmann W. Philos Mag A: Philos Mag A 1988;57:637.
[67] Dimitrakopulos G, Komminou Ph, Karakostas Th, Pond RC. Interf Sci 1999;7:217.
[68] Romanov AE, Vladimirov VI. In: Nabarro FRN, editor. Dislocations in solids, vol. 9. Amsterdam: North Holland; 1992. p. 191.
[69] Klimanek P, Klemm V, Romanov AE, Seefeldt M. Adv Eng Mater 2001;3:877.
[70] Kirchheim R. Acta Mater 2002;50:413.
[71] Gan Y, Zhou B. Scripta Mater 2001;45:625.
[72] Li H, Ebrahimi F. Adv Mater 2005;17:1969.
[73] Moser B, Hanlon T, Kumar KS, Suresh S. Scripta Mater 2006;54:1151.

[74] Rice JR, Thompson RM. Philos Mag 1974;29:73.
[75] Rice JR. J Mech Phys Solid 1992;40:239.
[76] Clery F, Yip S, Wolf D, Phillipot SR. Phys Rev Lett 1997;79:1309.
[77] Beltz GE, Lipkin DM, Fischer LL. Phys Rev Lett 1999;82:4468.
[78] Beltz GE, Fischer LL. Philos Mag A 1999;79:1367.
[79] Zhang TY, Li JCM. Acta Metall Mater 1991;39:2739.
[80] Beltz GE, Rice JR, Shih CF, Xia L. Acta Mater 1996;44:3943.
[81] Indenbom VI. Sov Phys Solid State 1961;3:1506.
[82] Smithells CJ, Brands EA. Metals reference book. London: Butterworth; 1976.
[83] Munro RG. J Am Ceram Soc 1997;80:1919.
[84] Lodziana Z, Norskov JK. J Chem Phys 2001;115:11261.